Published in final edited form as:
FEBS J. 2008 November ; 275(21): 5272–5285. doi:10.1111/j.1742-4658.2008.06655.x.

Role for nectin-1 in herpes simplex virus 1 entry and spread in human retinal pigment epithelial cells

Vaibhav Tiwari[1], **Myung-Jin Oh**[1], **Maria Kovacs**[1], **Shripaad Y. Shukla**[1], **Tibor Valyi-Nagy**[2], and **Deepak Shukla**[1,3]

[1] Department of Ophthalmology and Visual Sciences, College of Medicine, University of Illinois, Chicago, IL, USA

[2] Department of Pathology, College of Medicine, University of Illinois, Chicago, IL, USA

[3] Department of Microbiology and Immunology, College of Medicine, University of Illinois, Chicago, IL, USA

Abstract

Herpes simplex virus 1 (HSV-1) demonstrates a unique ability to infect a variety of host cell types. Retinal pigment epithelial (RPE) cells form the outermost layer of the retina and provide a potential target for viral invasion and permanent vision impairment. Here we examine the initial cellular and molecular mechanisms that facilitate HSV-1 invasion of human RPE cells. High-resolution confocal microscopy demonstrated initial interaction of green fluorescent protein (GFP)-tagged virions with filopodia-like structures present on cell surfaces. Unidirectional movement of the virions on filopodia to the cell body was detected by live cell imaging of RPE cells, which demonstrated susceptibility to pH-dependent HSV-1 entry and replication. Use of RT-PCR indicated expression of nectin-1, herpes virus entry mediator (HVEM) and 3-*O*-sulfotransferase-3 (as a surrogate marker for 3-O-sulfated heparan sulfate). HVEM and nectin-1 expression was subsequently verified by flow cytometry. Nectin-1 expression in murine retinal tissue was also demonstrated by immunohistochemistry. Antibodies against nectin-1, but not HVEM, were able to block HSV-1 infection. Similar blocking effects were seen with a small interfering RNA construct specifically directed against nectin-1, which also blocked RPE cell fusion with HSV-1 glycoprotein-expressing Chinese hamster ovary (CHO-K1) cells. Anti-nectin-1 antibodies and F-actin depolymerizers were also successful in blocking the cytoskeletal changes that occur upon HSV-1 entry into cells. Our findings shed new light on the cellular and molecular mechanisms that help the virus to enter the cells of the inner eye.

Keywords

actin cytoskeleton; filopodia; herpes simplex virus 1; human retinal pigment epithelial cells; nectin-1

Correspondence: D. Shukla, Department of Ophthalmology & Visual Sciences, 1855 West Taylor Street (M/C648), Chicago, IL 60612, USA, Fax: +1 312 996 7773, Tel: +1 312 355 0908, dshukla@uic.edu.

Supporting information

The following supplementary material is available:

Video S1. Surfing of HSV-1 (K26GFP) on filopodia. The video demonstrates unidirectional surfing of an HSV-1 (green) particle on a filopodium.

This supplementary material can be found in the online version of this article.

Please note: Wiley-Blackwell is not responsible for the content or functionality of any supplementary material supplied by the authors. Any queries (other than missing material) should be directed to the corresponding author for the article.

Herpes simplex virus 1 (HSV-1) entry into cells is a complex process that is initiated by specific interaction of viral envelope glycoproteins and host cell surface receptors [1–5]. Both HSV-1 and herpes simplex virus 2 (HSV-2) use glycoprotein B (gB) and glycoprotein C to mediate their initial attachment to cell surface heparan sulfate proteoglycans. Binding of herpesviruses to heparan sulfate proteoglycans probably precedes a conformational change that brings viral glycoprotein D (gD) to the binding domain of host cell surface gD receptors [6]. Thereafter, a concerted action involving gD, its receptor, three additional herpes simplex virus glycoproteins, gB, glycoprotein H (gH), and glycoprotein L (gL), and possibly an additional gB coreceptor trigger fusion of the viral envelope with the plasma membrane of host cells [7]. Subsequently, viral capsids and tegument proteins are released into the cytoplasm of the host cell.

The gD receptors include cell surface molecules derived from three structurally unrelated families. These include herpes virus entry mediator (HVEM), a member of the tumor necrosis factor receptor family [8], nectin-1 and nectin-2, which belong to the immunoglobulin superfamily [9–12], and a modified form of heparan sulfate, 3-O-sulfated heparan sulfate (3-OS HS) [2,10,13–15]. HVEM principally mediates entry of HSV-1 into human T lymphocytes and trabecular meshwork cells, and is expressed in many fetal and adult human tissues, including the lung, liver, kidney, and lymphoid tissues [7,8,16]. HVEM also mediates HSV-2 entry into human corneal fibroblasts [17]. Nectin-1 and nectin-2 mediate entry of HSV-1 and HSV-2, but the HSV-1 entry-mediating activity of nectin-2 is limited to some mutant strains only [7,12]. Nectin-1 is extensively expressed in human cells of epithelial and neuronal origin [18], whereas nectin-2 is widely expressed in many human tissues, but has only limited expression in neuronal cells and keratinocytes [7]. The nonprotein receptor 3-OS HS is expressed in multiple human cell lines (e.g. neuronal and endothelial cells) and mediates entry of HSV-1, but not HSV-2 [2,13,19].

Retinitis and acute retinal necrosis (ARN) caused by HSV-1 infection result in severe complications in patients [20–23]. ARN is a blinding disease marked by rapidly progressive peripheral retinal necrosis. HSV-1 appears to be the second most common cause of ARN [24]. It is postulated that ARN caused by herpes simplex virus may be the result of recurrence of a previous episode of retinitis caused by the virus [25]. The disease is typically characterized by inflammatory orbitopathy, proptosis, and optic nerve involvement. Immunohistochemical studies have detected HSV-1 antigens in the retinal periphery [26].

In an effort to determine a mechanism for HSV-1 in retinal damage, specifically in terms of its ability to enter the cells of the retina, the present study used retinal pigment epithelial (RPE) cells as a model to determine the susceptibility and the mediators of HSV-1 entry into these cells. Using multiple assays, we demonstrate some unique aspects of the virus attachment to RPE cells and consequent changes in the host cytoskeleton. We also demonstrate that nectin-1 is a major determinant of HSV-1 entry into RPE cells. In addition, nectin-1 can influence cell-to-cell spread of the virions involving membrane fusion.

Results

Attachment of HSV-1 to cell membrane of RPE cells

In order to study the initial interaction of HSV-1 virions with cells, live cell imaging was performed. Green fluorescent protein (GFP)-tagged HSV-1 virions (K26GFP) [27] were added to RPE cells plated at a low population density. Our time lapse images demonstrated that many virions directly reached the cell body, whereas many others first attached to filopodia-like projections present on the plasma membrane of RPE cells (Video S1). The viral movements in culture solutions were random until the virus particles made contact with the cells. Quite noticeably, some virus particles that initially attached to filopodia were able to travel

unidirectionally along the filopodia to reach the cell body (Video S1). The virus movement highlighted had an average speed of 1.5 $\mu m \cdot min^{-1}$. These movements on filopodia mimic the surfing phenomenon reported with retroviruses [28], and are also seen with many other cell types. The average speed of viral movements on filopodia matches that of the F-actin retrograde flow, and it is not affected by plating density (Oh and Shukla, unpublished results). Attachment of K26GFP [27] to filopodia was also noticeable in fixed cells stained for F-actin (red) (Fig. 1).

HSV-1 entry into cultured human RPE cells

To compare the abilities of cultured RPE cells to support HSV-1 entry, confluent monolayers of RPE, HeLa, Vero and naturally resistant Chinese hamster ovary-K1 (CHO-K1) cells were plated in a 96-well plate and infected with identical dilutions of recombinant HSV-1(KOS) tk12 [12], which expresses β-galactosidase upon entry into cells. The entry of HSV-1 was measured after 6 h of viral infection, using a colorimetric assay [13]. As shown in Fig. 2A, there was significantly more entry into RPE cells than in CHO-K1 cells, and the absorbance (*A*) signals representing entry into RPE cells were very similar to those seen with HeLa and Vero cells. Both HeLa and Vero cell are naturally susceptible and frequently used for examining entry and virus propagation. Similar results were obtained when individual cells were examined for HSV-1 entry using an insoluble substrate, 5-bromo-4-chloro-3-indolyl-β-D-galactopyranoside (X-gal). As expected, virtually no β-galactosidase activity was observed in CHO-K1 cells (Fig. 2B, bottom panel), while a dosage of virus sufficient to infect 100% of nectin-1 CHO cells (Fig. 2B, top and middle panels) was also sufficient for nearly complete infection of RPE cells.

Effect of pH on HSV-1 entry into RPE cells

We also examined the pH dependence of HSV-1 entry into RPE cells. It had been previously reported that HSV-1 entry into some cell types can be pH-dependent and inhibition of vesicular acidification can inhibit entry [29,30]. Thus, the impacts of lysosomotropic agents that interfere with vesicular acidification were tested at previously published concentrations [29,30]. These include bafilomycin A1 (BFLA-1) [27,28,30], chloroquine, and NH_4Cl [31]. Monolayer cultures of RPE cells were pretreated with BFLA-1 (Fig. 2C) or either chloroquine or NH_4Cl (Fig. 2D). There was very strong dose-dependent inhibition of HSV-1 entry into RPE cells by all three lysosomotropic agents examined (Fig. 2). Chloroquine, BFLA-1 and NH_4Cl all inhibited entry, with up to 80% inhibition being seen at the highest concentrations, demonstrating pH dependence of HSV-1 entry into RPE cells.

Visual and quantitative analyses of HSV-1 replication in cultured RPE cells

Because HSV-1 was able to enter cultured RPE cells, we next evaluated whether entry leads to active virus production. Initially, fluorescence microscopy was used to obtain visual evidence of HSV-1 replication and virion production. K26GFP [27] was used for infecting cultured RPE cells, and the virus was allowed to replicate. Cells were fixed at different time points and stained for F-actin (red). The GFP intensity (representing virus production) increased significantly over time, as seen pictorially in Fig. 3A–E and in graphical form in Fig. 3F. Infection usually spread to neighboring cells in clusters, and many individual cells remained uninfected. Furthermore, to assess viral replication, the ability of HSV-1 to form plaques in RPE cells was analyzed. As shown in Fig. 3G–L, cultured RPE cells exposed to HSV-1 (KOS804) at a multiplicity of infection (MOI) of 0.01 produced a larger number of plaques over time. The plaque sizes increased over time (Fig. 3G–K), and so did the number of plaques formed (Fig. 3L). These results, together with those of the entry assay and visualization of GFP-tagged HSV-1, show that entry of HSV-1 into cultured RPE leads to a productive infection.

Identification of gD receptors expressed in cultured RPE cells

RT-PCR analysis was performed to determine the identity of gD receptors expressed in RPE cells. Specific primers for HVEM, nectin-1, nectin-2 and 3-*O*-sulfotransferase-3 (3-OST-3) were used. As shown in Fig. 4A, products of the expected size for all these receptors were detected. To further analyze the cell surface expression of gD receptors, flow cytometry was performed. As nectin-2 does not mediate entry of wild-type HSV-1 [12], it was not included in flow cytometry experiments. HVEM-expressing CHO-K1 cells (control) and RPE cells were positive for HVEM expression (Fig. 4B). Similarly, nectin-1-expressing CHO-K1 cells and also RPE cells were positive for nectin-1 (Fig. 4C). However, 3-OS HS expression was undetectable (data not shown). In order to verify our receptor expression findings *in vivo*, immunohistochemistry was performed using sections of retina obtained from adult (8 months old) female BALB/c mice. As shown in Fig. 4D, strong nectin-1 expression (brown) was detected in the retinal epithelium. HVEM staining was weak, and no clear signals were reported for 3-OS HS (data not shown). Thus it is likely that nectin-1 and/or HVEM could be important for HSV-1 entry into RPE cells.

Nectin-1 acts as the major receptor for HSV-1 entry into RPE cells

To determine which receptors were important for HSV-1 entry into RPE cells, previously established receptor-specific antibodies were used [8,9,18]. As shown in Fig. 5A, only antibody against nectin-1, in a dose-dependent manner, demonstrated inhibition of HSV-1 entry. At the highest dose, the antibody was able to block approximately 90% of HSV-1 entry (Fig. 5A). In contrast, antibodies against HVEM and 3-OS HS failed to significantly affect virus entry. The role of nectin-1 was also assessed by RNA interference assay. A commercially validated small interfering RNA (si-RNA) construct against nectin-1, but not its scrambled control, was able to inhibit over 80% of HSV-1 entry into RPE cells (Fig. 5B). The inhibition was probably due to downregulation of nectin-1 from RPE cells by nectin-1-specific si-RNA construct (Fig. 5C).

As the entry receptor can also play a role in viral spread by mediating cell-to-cell fusion [32, 33], we also decided to examine the role of nectin-1 in the fusion of RPE cells with viral glycoprotein-expressing cells. In a semiquantitative, luciferase-based cell fusion assay [33], the RPE cells that were downregulated for nectin-1 expression demonstrated about 75% less fusion than corresponding control RPE cells transfected with scrambled si-RNAs (Fig. 6A). A similar result was obtained when the cells were allowed to form syncytia. Significantly fewer syncytia were seen with RPE cells that had downregulated nectin-1 expression (Fig. 6B, right panel) than with the control (Fig. 6B, left panel).

Cytoskeleton rearrangements in RPE cells during HSV-1 infection

Our previous findings have shown that HSV-1 entry into corneal fibroblasts (CFs) leads to changes in actin cytoskeleton [29]. We also decided to examine whether cytoskeletal changes played any significant role in HSV-1 entry into RPE cells. To address this issue, we used chemical agents such as cytochalasin D (Cyto D) [34–36] and latrunculin A (Lat A) [7]. Both can prevent cytoskeletal changes by preventing actin polymerization. Cyto D and Lat A caused dose-dependent inhibition of HSV-1 entry into RPE cells (Fig. 7A,B). The agents were able to block up to 80% of HSV-1 entry into RPE cells, suggesting that significant changes in the cytoskeleton may be needed during the initial phase of HSV-1 infection. Furthermore, as the chemical agents may have some unknown effects on β-galactosidase readout, we also decided to visualize changes in the cytoskeleton that may occur during the initial 6 h window of infection. We infected RPE cells with K26GFP [27], and stained cells for F-actin, using phalloidin at 30 min and 6 h postinfection, and examined the cells under a high-resolution confocal microscope (Fig. 7C). Two changes were frequently observed: cells at 30 min of infection produced higher numbers of filopodia with virus attached to them (Fig. 7Ca–c), and many cells at 6 h postinfection formed distinct stress fibers (Fig. 7Cd–f). These stress fibers,

but not so much filopodia formation, could be prevented by pretreating the RPE cells with antibody against nectin-1 (Fig. 7Cg,h). It is likely that pretreatment of cells with monoclonal antibody against nectin-1 (PRR1) also negatively affects virus attachment to cells (Fig. 7Ci). Overall, our data support an important role for nectin-1 in RPE cell infection.

Discussion

We began this study with the goal of analyzing the ability of HSV-1 to enter RPE cells. We were able to complete a systematic study that revealed several interesting features of entry. Our study is the first of its kind demonstrating live cell imaging of the attachment of the virions to RPE cells (Fig. 1). It implicates viral surfing on filopodia as a means for targeted delivery of the virions to the cell body. Additionally, we demonstrated the pH dependence of viral uptake by RPE cells (Fig. 2), identified entry receptors that are expressed by RPE cells (Fig. 4), and specifically implicated nectin-1 as the major receptor for entry and also for cell-to-cell spread (Figs 4–6). Our demonstration of the expression of nectin-1 in the murine retina (Fig. 4) suggests a possible correlation of our in vitro findings *in vivo*. We also highlighted the changes in the actin cytoskeleton and their possible association with entry and infection mediated by nectin-1 (Fig. 7).

Our study adds to the growing body of evidence that the mode of entry and receptor usage can be cell-type-specific [29,30]. Although nectin-1 is probably important for the infection of neuronal tissues [10,37,38], cells of ocular origin, such as CFs and trabecular meshwork cells, do not seem to express nectin-1 [15,16]. RPE cells appear to comprise one of the first ocular cell types that not only expresses nectin-1 but also utilizes it as a major receptor for entry. The presence of nectin-1 on RPE cells and its absence on CFs and trabecular meshwork cells may be explicable by considering that RPE cells are closer to the optic nerve and are derived from the neuroectoderm. Most tissues of neuronal origin tend to express nectin-1 [10,18].

The discovery of nectin-1 as the major mediator of entry into RPE cells may also be important, because herpes simplex virus-induced ARN is often seen in patients with a history of central nervous system disease [39]. Our results indicate that nectin-1 could possibly play a role in cell-to-cell viral spread during primary infection (Figs 4–6) and may be instrumental in the virus's ability to reach trigeminal ganglia for the establishment of latency. Because the virus reactivates in the nervous system, it is tempting to speculate that the development of ARN after a previous infection with herpes simplex virus may also be mediated by nectin-1 [21,39–43]. Although the significance of nectin-1 in reactivated viral spread is yet to be defined, our study presents a strong case for focusing on nectin in reactivated diseases caused by both HSV-1 and HSV-2 [22]. The demonstration of nectin-1 expression in the retina can also provide useful information on its normal physiological significance as a cell adhesion molecule and its significance in vision processing. Similarly, the discovery that entry could be significantly decreased by increasing the pH of intracellular vesicles (Fig. 2) raises some interesting possibilities for the actual mechanism by which the virus is able to travel from the cell membrane to the nucleus. A similar effect was observed in CFs and keratinocytes [29,30]. A pH dependence for the formation of polykaryons by herpes simplex virus has also been observed [44]. Thus, our study identifies yet another, natural target cell type that probably uses endocytosis for virus uptake and entry, and in which lysosomotropic agents can be tested for efficacy in blocking viral spread during ARN *in vivo*.

An important aspect of viral infection is how the pathogen can cause damage to cells. One likely area for the virus to affect is the host actin cytoskeleton, as observed in this study and reported previously [29]. Clearly, the virus can cause cells to change drastically, and the changes in the cytoskeleton can be observed as early as a few minutes after infection (Fig. 7). As blocking of nectin-1 can prevent changes in the cytoskeleton, it is likely that either most

changes are induced postentry before entry with the involvement of nectin-1. An interesting finding of the current study is that F-actin synthesis can be important for entry, as actin depolymerizers block infection (Fig. 7). Could it be that filopodia or similar membrane protrusions that are rich in F-actin form a crucial part of viral uptake? We have recently found evidence to suggest that phagocytosis-like uptake is exploited for viral entry into nectin-1-expressing CHO-K1 cells and CFs [29]. Another use of F-actin-rich membrane projections may be related to surfing on filopodia (Fig. 1) that might be conserved among unrelated viruses [28]. Expression of nectin-1 on filopodia has been demonstrated, with possible functional implications for the regulation of filopodia formation [45]. Thus, it is likely that F-actin cytoskeletal changes may be related to enhanced and more productive viral infection, and the interaction of the virus with nectin-1 may play a critical role in regulating the actin cytoskeleton to favor the entry process. Given that much work still needs to be done to fully understand HSV-1 infection of all target cells, including RPE cells, our study provides new starting points for understanding viral pathogenesis in the retina and advancing novel therapies to control retinal infection by HSV-1.

Experimental procedures

Cells and viruses

RPE cells were provided by B. Y. J. T. Yue (University of Illinois at Chicago). P. G. Spear (Northwestern University, Chicago) provided wild-type CHO-K1 cells and many of the viruses used throughout this study. Wild-type CHO-K1 cells were grown in Ham's F12 (Invitrogen Corp., Carlsbad, CA, USA) supplemented with 10% fetal bovine serum, and African green monkey kidney (Vero) cells were grown in DMEM (Invitrogen) supplemented with 5% fetal bovine serum. Cultures of RPE cells were grown in L-glutamine-containing DMEM (Invitrogen) supplemented with 10% fetal bovine serum. Cells were trypsinized and passaged after reaching confluence. Recombinant β-galactosidase-expressing HSV-1(KOS) tk12 [12] and HSV-1(KOS) gL86 [13] were used. GFP-expressing HSV-1 (K26GFP) [27] was provided by P. Desai (Johns Hopkins University, Baltimore). The viral stocks were propagated in complementing cell lines, titered on Vero cells, and stored at −80 °C.

Live virus cell imaging

RPE cells were imaged using a 100× oil (Plan-APO 1.4) objective on an inverted microscope (Eclipse TE2000). Cells were plated on 35 mm glass-bottomed dishes (Mattek Corp., Ashland, MA, USA) coated with collagen (BD Biosciences, San Jose, CA, USA). Cells were washed with NaCl/P_i and were placed in serum-free Optimem (Invitrogen) just prior to imaging. K26GFP was added to cells at an MOI of 20, and RPE cells were imaged every 10 s (Eclipse TE2000; Nikon Corp., Tokyo, Japan), using both a bright field and GFP channel after the addition of virus. Video frames were shown at 10 frames per second. All images and videos were processed by METAMORPH (Molecular Devices) and PHOTOSHOP (Adobe Systems Inc., San Jose, CA, USA).

Viral entry assay

Viral entry assays were based on quantitation of β-galactosidase expressed from the viral genome or by CHO-IEβ8 cells in which β-galactosidase expression is inducible by herpes simplex virus infection [13]. Cells were washed and exposed to serially diluted virus in 50 μL of NaCl/P_i containing 0.1% glucose and 1% heat-inactivated bovine serum (NaCl/P_i-G-BS) for 6 h at 37 °C before solubilization in 100 μL of NaCl/P_i containing 0.5% NP-40 and the β-galactosidase substrate *o*-nitrophenyl-β-D-galactopyranoside (ONPG; ImmunoPure, Pierce, Rockford, IL, USA; 3 mg-mL^{-1}). The enzymatic activity was monitored at 410 nm by spectrophotometry (Molecular Devices spectra MAX 190, Sunnyvale, CA, USA) at several time points after the addition of ONPG in order to define the interval over which the generation

of the product was linear with time. Herpes simplex virus entry into RPE cells was also confirmed by X-gal staining. The RPE cells were grown in Lab-Tek chamber slides. After 6 h of infection with reporter virus, cells were washed with NaCl/P_i and fixed with 2% formaldehyde and 0.2% glutaradehyde at room temperature for 15 min. The cells were then washed with NaCl/P_i and permeabilized with 2 mm $MgCl_2$, 0.01% deoxycholate and 0.02% Nonidet NP-40 for 15 min. After rinsing with NaCl/P_i, 1.5 mL of 1.0 mg·mL^{-1} X-gal in ferricyanide buffer was added to each well, and the blue color developed in the cells was examined. Microscopy was performed using the 20× objective of the inverted microscope (Zeiss, Axiovert 100M). slide book version 3.0 was used for images. All experiments were repeated a minimum of three times unless otherwise noted.

Fluorescent microscopy of viral replication

Cultured monolayers of RPE cells (approximately 10^6) were grown overnight in DMEM on chamber slides (Lab-Tek). The cells were infected with K26GFP at 0.01 MOI in serum-free media, and this was followed by fixation of cells at given time points (0, 24, 36, 48 and 60 h postinfection) using fixative buffer (2% formaldehyde and 0.2% glutaradehyde). The cells were then washed with NaCl/P_i and permeabilized with 2 mm MgCl2, 0.01% deoxycholate and 0.02% Nonidet NP-40 for 20 min. After rinsing with NaCl/P_i, 10 nm rhodamine-conjugated phalloidin (Invitrogen) was added for F-actin staining at room temperature for 45 min. Finally, the cells were washed three times with 1× NaCl/P_i before microscopy was performed using the 20× objective of the inverted microscope (Zeiss, Axiovert 100M). In a parallel experiment, RPE cells were grown in 96-well plates, and the GFP intensity of HSV-1-infected RPE cells was quantified with a TeCan spectrophotometer.

Plaque assay

Confluent layers of RPE cells (approximately 10^6) in six-well dishes were infected with HSV-1 (804) at 0.01 plaque-forming units (PFU) per cell or mock-infected for 2 h at 37 °C. After removal of inocula, monolayers were overlaid with DMEM containing 2.5% heat-inactivated fetal bovine serum and incubated at 37 °C. At different time points (0, 24, 36, 48 and 60 h), the cells were fixed by using fixative buffer (2% formaldehyde and 0.2% glutaradehyde) at room temperature for 20 min, and then stained with Giemsa for 45 min. The cells were again washed five times in NaCl/P_i, and the numbers of plaques were counted. The images were taken with a Zeiss Axiovert 100 microscope.

Virus-free cell-to-cell fusion assay

In this experiment, the CHO-K1 cells (grown in F-12 Ham; Invitrogen) designated as ‘effector’ cells were cotransfected with plasmids expressing four HSV-1(KOS) glycoproteins, pPEP98 (gB), pPEP99 (gD), pPEP100 (gH) and pPEP101 (gL), along with plasmid pT7EMCLuc, which expresses the firefly luciferase gene under the T7 promoter [14]. Wild-type CHO-K1 cells express cell surface heparan sulfate but lack functional gD receptors, including 3-OS HS [19]. As a result, they are resistant to both herpes simplex virus entry and virus-induced cell fusion [2,14]. Cultured RPE cells considered as ‘target cells’ were cotransfected with pCAGT7, which expresses T7 RNA polymerase using chicken actin promoter and cytomegalovirus enhancer [14]. The effector cells expressing pT7EMCLuc and pCDNA3 (devoid of any glycoproteins) and the target RPE cells transfected with T7 RNA polymerase were used as the control. For fusion, at 18 h post-transfection, the target and the effector cells were mixed together (1 : 1 ratio) and cocultivated in 24-well dishes. The activation of the reporter luciferase gene as a measure of cell fusion was examined using a reporter lysis Assay (Promega) at 24 h postmixing. In a parallel experiment, the target RPE cells were transfected with enhanced GFP plasmid, and the effector CHO-K1 cells expressing HSV-1 glycoproteins were transfected with red plasmid (DS-Red; BD Biosciences). At 18 h postmixing, the cells were fixed and

permeabilized, and this was followed by F-actin staining with 10 nM rhodamine-conjugated phalloidin (Invitrogen). The images were taken with a Zeiss Axiovert 100 microscope.

Detection of gD receptors by RT-PCR

Total RNA was isolated from the cultured RPE cells using a Qiagen RNeasy kit (Qiagen Corp., Valencia, CA, USA). SUPERSCRIPT II RT (Invitrogen) was used for RT-PCR. PCR amplification of cDNAs was performed with the following primers: 5′-TCTCTGCTGC CAGACA-3′ and 5′-GCCACAGCAGAACAGA-3′ for HVEM; 5′-TCCTTCACCGATGGCACTATCC-3′ and 5′-TCAACACCAGCAGGATGCTC-3′ for nectin-1; and 5′-AGAAGCAGCAGCACCAGCAG-3′ and 5′-GTCACGTTCAGCCAGGA-3′ for nectin-2. The 3-OST-3 sequences were amplified using 5′-CAGGCCATCATCATCGG-3′ and 5′-CCGGTCATCTGGTAGAA-3′ primers. RT-PCR analysis was performed as described previously. The expected sizes of the PCR products were 1270 bp for HVEM, 738 bp for nectin-1, 616 bp for nectin-2, and 736 bp for 3-OST-3, respectively. HeLa cell cDNAs that are known to express herpes simplex virus entry receptors were used a positive control.

Flow cytometry analysis

For cell surface expression of HVEM and nectin-1 receptor, flow cytometery analysis was performed. Unless indicated otherwise, monolayers of approximately 5×10^6 RPE cells were incubated at 4 °C for 45 min with monoclonal antibodies against HVEM (1 : 200) (Cat. no. sc-74089; Santa Cruz Biotechnologies, Santa Cruz, CA, USA) and nectin-1 (1 : 100) (Cat. no. R1.302.12; Beckman Coulter, Fullerton, CA, USA) [9]. The antibody against 3-OS-HS was kindly provided by T. Kuppevelt (Radboud University, The Netherlands). RPE cells stained with only fluorescein isothiocyanate (FITC)-conjugated secondary anti-(mouse IgG) were used as background controls. Cells were examined by fluorescence-activated cell sorter (FACS) analysis after 50 min of incubation with FITC-conjugated secondary anti-(mouse IgG) (1 : 500).

Antibody blocking assay

Antibody blocking assay was performed as previously described [16]. RPE cells plated in 96-well plates were preincubated at room temperature with twofold dilutions of previously described antibodies against HVEM [8] and nectin-1 (PRR1) [9] for 90 min. Cells were then challenged with identical doses of HSV-1 (gL86) at 5×10^5 PFU per well at 37 °C. After 6 h, the cells were washed twice with NaCl/P_i and treated for 1 min with 0.1 M citrate buffer (pH 3.0). The substrate, ImmunoPure ONPG (3 mg·mL^{-1}; Pierce), was prepared in NaCl/P_i (Invitrogen) with nonionic detergent (120 μL of 1% Igepal CA-630; Sigma, St Louis, MO, USA), and β-galactosidase activity was read at 410 nm. The experiment was repeated three times, with similar results.

Effect of pH on HSV-1 entry into RPE cells

To support pH-dependent entry, the effects of lysosomotropic agents on entry of herpes simplex virus into RPE cells were examined. Monolayer cultures of RPE cells (approximately 10^6 cells) cultured in a 96-well plate were pretreated with the indicated concentrations of agents for 1 h at room temperature: BFLA-1, choloroquine, and NH_4Cl (Sigma), or mock treated as a control. The stocks of the reagents were prepared in NaCl/P_i. Cells were infected with *lacZ*$^+$ HSV-1 (KOS) (gL86) at 50 PFU per cell for 6 h at 37 °C. An ONPG entry assay was performed to estimate the enzymatic activity at 410 nm by spectrophotometry (Molecular Devices spectra MAX 190, Sunnyvale, CA, USA).

Effect of actin-depolymerizing agents on HSV-1 entry into RPE cells

In order to demonstrate the significance of the actin cytoskeleton network during HSV-1 entry into RPE cells, the effects of actin-depolymerizing agents on entry of herpes simplex virus into RPE cells were examined. Monolayer cultures of RPE cells (approximately 10^6 cells) in a 96-well plate were pretreated with the indicated concentrations of agents for 1 h at room temperature: Cyto D and Lat A (Sigma), or mock treated as a control. The stocks of the reagents were prepared in NaCl/P_i. Cells were infected with *lacZ*$^+$ HSV-1(KOS) (gL86) at 50 PFU per cell for 6 h at 37 °C. An ONPG entry assay was performed to estimate the enzymatic activity at 410 nm by spectrophotometry.

Immunohistochemistry

Tissue sections were hydrated with distilled water, and antigen retrieval was performed using DAKO Target Retrieval Solution 10× concentrate (DAKO, Carpinteria, CA, USA). Nonspecific staining was blocked using an H_2O_2 solution for 10 min, followed by a protein block for 10 min. Sections were incubated with nectin-1-specific antiserum R166 (1 : 50) at room temperature for 1 h. Nectin-1 staining was detected using the DAKO Envision$^+$ kit. For rat retinal tissue, the following method was used. The posterior eyecups were fixed in 4% paraformaldehyde in 0.1 M Sorenson's phosphate buffer (PB; pH 7.4) for 20 min at room temperature, washed four times in PB, and cryoprotected by stepping through 10%, 20% and 30% sucrose overnight at 4 °C. The tissue was then embedded in OCT, sectioned at 10 μm, and mounted on Superfrost plus slides (Fisher, Pittsburgh, PA, USA). Retinal sections were stained with a primary antibody for 48 h at 4 °C (a polyclonal antibody directed against the nectin-1 receptor, 1 : 100), and then incubated for 40 min incubation with the secondary antibodies [Alexa Fluor 546 goat anti-(rabbit IgG), 1 : 200; Invitrogen, Carlsbad, CA, USA]. Nuclei were labeled with TO-PRO-3 iodide (Invitrogen) at a final concentration of 5 μm in the mounting medium (Vectashield H-1000; Jackson ImmunoResearch Laboratory, West Grove, PA, USA). Confocal and differential interference contrast image acquisition was conducted with an SB2-AOBS confocal microscope (Leica, Solms, Germany).

Effect of siRNA against nectin-1 on HSV-1 entry into RPE cells

siRNAs that downregulate nectin-1 (SASI-HS01-00046268; Sigma) were used in RPE cells to interfere with receptor expression. RPE cells were plated onto a six-well tissue culture dish, and were transfected with the RNA duplexes or control scrambled RNA duplexes. After 24 h, cells were loosened with Cell Dissociation Buffer (Invitrogen) and replated onto 96-well tissue culture dishes. Viral entry assays were performed as previously described with serial dilutions of HSV-1(KOS) gL86. As stated before, a spectrophotometer (Molecular Devices) was used to measure β-galactosidase activity at 410 nm.

Statistical analysis

Data are expressed as mean ± SD and were analyzed statistically by using one-way ANOVA tests. $P < 0.05$ was considered to be statistically significant.

Supplementary Material

Refer to Web version on PubMed Central for supplementary material.

Acknowledgments

This work was supported by National Institute of Health (NIH) grants Al057860 (D. Shukla) P30EY001792 (core), and a Research to Prevent Blindness career award (D. Shukla). V. Tiwari was supported by an American Heart Association (AHA) postdoctoral fellowship (AHA0525768Z) and a grant award from the Illinois Society for Prevention of Blindness (ISPB).

References

1. Liu J, Throp SC. Cell surface heparan sulfate and its roles in assisting viral infections. Med Res Rev 2002;22:1–25. [PubMed: 11746174]
2. Shukla D, Spear PG. Herpesviruses and heparan sulfate: an intimate relationship in aid of viral entry. J Clin Invest 2001;108:503–510. [PubMed: 11518721]
3. Shieh MT, WuDunn D, Montgomery RI, Esko JD, Spear PG. Cell surface receptors for herpes simplex virus are heparan sulfate proteoglycans. J Cell Biol 1992;116:1273–1281. [PubMed: 1310996]
4. Spillmann D. Heparan sulfate: anchor for viral intruders? Biochimie 2001;83:811–817. [PubMed: 11530214]
5. WuDunn D, Spear PG. Initial interaction of herpes simplex virus with cells is binding to heparan sulfate. J Virol 1989;63:52–58. [PubMed: 2535752]
6. Krummenacher C, Baribaud I, Ponce de Leon M, Whitbeck JC, Lou H, Cohen GH, Eisenberg RJ. Localization of a binding site for herpes simplex virus glycoprotein D on herpesvirus entry mediator C by using antireceptor monoclonal antibodies. J Virol 2000;74:10863–10872. [PubMed: 11069980]
7. Spear PG, Longnecker R. Herpesvirus entry: an update. J Virol 2003;77:10179–10185. [PubMed: 12970403]
8. Montgomery RI, Warner MS, Lum BJ, Spear PG. Herpes simplex virus-1 entry into cells mediated by a novel member of the TNF/NGF receptor family. Cell 1996;87:427–436. [PubMed: 8898196]
9. Cocchi F, Menotti L, Mirandole P, Lopez M, Campadelli-Fumi G. The ectodomain of a novel member of the immunoglobulin subfamily related to the poliovirus receptor has the attributes of a bona fide receptor for herpes simplex virus types 1 and 2 in human cells. J Virol 1998;72:9992–10002. [PubMed: 9811737]
10. Shukla D, Dal Canto MC, Rowe CL, Spear PG. Striking similarity of murine nectin-1alpha to human nectin-1alpha (HveC) in sequence and activity as a glycoprotein D receptor for alphaherpesvirus entry. J Virol 2000;74:11773–11781. [PubMed: 11090177]
11. Spector I, Shochet NR, Blasberger D, Kashman Y. Latrunculins – novel marine macrolides that disrupt microfilament organization and affect cell growth: I. Comparison with cytochalasin D. Cell Motil Cytoskeleton 1989;13:127–144. [PubMed: 2776221]
12. Warner MS, Geraghty RJ, Martinez WM, Montgomery RI, Whitbeck JC, Xu R, Eisenberg RJ, Cohen GH, Spear PG. A cell surface protein with herpesvirus entry activity (HveB) confers susceptibility to infection by mutants of herpes simplex virus type 1, herpes simplex virus type 2, and pseudorabies virus. Virology 1998;246:179–189. [PubMed: 9657005]
13. Shukla D, Liu J, Blaiklock P, Shworak NW, Bai X, Esko JD, Cohen GH, Eisenberg RJ, Rosenberg RD, Spear PG. A novel role for 3-*O*-sulfated heparan sulfate in herpes simplex virus 1 entry. Cell 1999;99:13–22. [PubMed: 10520990]
14. Tiwari V, Clement C, Duncan MB, Chen J, Liu J, Shukla D. A role for 3-*O*-sulfated heparin sulfate in cell fusion induced by herpes simplex virus type 1. J Gen Virol 2004;85:805–809. [PubMed: 15039523]
15. Tiwari V, Clement C, Xu D, Valyi-Nagy T, Yue BY, Liu J, Shukla D. Role for 3-O-sulfated heparan sulfate as the receptor for herpes simplex virus type 1 entry into primary human corneal fibroblasts. J Virol 2006;80:8970–8980. [PubMed: 16940509]
16. Tiwari V, Clement C, Scanlan PM, Kowlessur D, Yue BY, Shukla D. A role for herpesvirus entry mediator as the receptor for herpes simplex virus 1 entry into primary human trabecular meshwork cells. J Virol 2005;79:13173–13179. [PubMed: 16189018]
17. Tiwari V, Shukla SY, Yue BY, Shukla D. Herpes simplex virus type 2 entry into cultured human corneal fibroblasts is mediated by herpesvirus entry mediator. J Gen Virol 2007;88:2106–2110. [PubMed: 17622611]
18. Shukla D, Scanlan PM, Tiwari V, Sheth V, Clement C, Guzman-Hartman G, Dermody TS, Valyi-Nagy T. Expression of nectin-1 in normal and herpes simplex virus type 1-infected murine brain. Appl Immunohistochem Mol Morphol 2006;14:341–347. [PubMed: 16932027]
19. Tiwari V, ten Dam GB, Yue BY, van Kuppevelt TH, Shukla D. Role of 3-O-sulfated heparan sulfate in virus-induced polykaryocyte formation. FEBS Lett 2007;18:4468–4472. [PubMed: 17765228]

20. Atherton SS. Acute retinal necrosis: insights into pathogenesis from the mouse model. Herpes 2001;8:69–73. [PubMed: 11867023]
21. Kim C, Yoon YH. Unilateral acute retinal necrosis occurring 2 years after herpes simplex type 1 encephalitis. Ophthalmic Surg Lasers 2002;33:250–252. [PubMed: 12027110]
22. Lau CH, Missotten T, Salzmann J, Lightman SL. Acute retinal necrosis: features, management, and outcomes. Ophthalmology 2007;114:756–762. [PubMed: 17184841]
23. Uninsky E, Jampol LM, Kaufman S, Naraqi S. Disseminated herpes simplex infection with retinitis in a renal allograft recipient. Ophthalmology 1983;90:175–178. [PubMed: 6343943]
24. Muthiah MN, Michaelides M, Child CS, Mitchell SM. Acute retinal necrosis: a national population-based study to assess the incidence, methods of diagnosis, treatment strategies and outcomes in the UK. Br J Ophthalmol 2007;91:1452–1455. [PubMed: 17504853]
25. Duker JS, Nielsen JC Jr, Eagle RC, Bosley TM, Granadier R, Benson WE. Rapidly progressive acute retinal necrosis secondary to herpes simplex virus, type 1. Ophthalmology 1990;97:1638–1643. [PubMed: 1965022]
26. Kashiwase M, Sata T, Yamauchi Y, Minoda H, Usui N, Iwasaki T, Kurata T, Usui M. Progressive outer retinal necrosis caused by herpes simplex virus type 1 in a patient with acquired immunodeficiency syndrome. Ophthalmology 2000;107:790–794. [PubMed: 10768344]
27. Desai P, Person S. Incorporation of the green fluorescent protein into the herpes simplex virus type 1 capsid. J Virol 1998;72:7563–7568. [PubMed: 9696854]
28. Lehman MJ, Sherer NM, Marks CB, Pypaert M, Mothes W. Actin- and myosin-driven movement of viruses along filopodia precedes their entry into cells. J Cell Biol 2005;170:317–325. [PubMed: 16027225]
29. Clement C, Tiwari V, Scanlan PM, Valyi-Nagy T, Yue BY, Shukla D. A novel role for phagocytosislike uptake in herpes simplex virus entry. J Cell Biol 2006;174:1009–1021. [PubMed: 17000878]
30. Nicola AV, McEvoy AM, Straus SE. Roles for endocytosis and low pH in herpes simplex virus entry into HeLa and Chinese hamster ovary cells. J Virol 2003;77:5324–5332. [PubMed: 12692234]
31. de Duve C, de Barsy T, Poole B, Trouet A, Tulkens P, Van Hoof F. Lysosomotropic agents. Biochem Pharmacol 1974;23:2495–2531. [PubMed: 4606365]
32. Browne H, Bruun B, Minson T. Plasma membrane requirements for cell fusion induced by herpes simplex virus type 1 glycoproteins gB, gD, gH and gL. J Gen Virol 2001;82:1419–1422. [PubMed: 11369886]
33. Pertel PE. Human herpesvirus 8 glycoprotein B (gB), gH, and gL can mediate cell fusion. J Virol 2002;76:4390–4400. [PubMed: 11932406]
34. Gottlieb TA, Ivanov IE, Adesnik M, Sabatini DD. Actin microfilaments play a critical role in endocytosis at the apical but not the basolateral surface of polarized epithelial cells. J Cell Biol 1993;120:695–710. [PubMed: 8381123]
35. Rabinovitch M. Professional and non-professional phagocytes: an introduction. Trends Cell Biol 1995;5:85–87. [PubMed: 14732160]
36. Schafer DA. Regulating actin dynamics at membranes: a focus on dynamin. Traffic 2004;5:463–469. [PubMed: 15180823]
37. Guzman G, Oh S, Shukla D, Engelhard HH, Valyi-Nagy T. Expression of entry receptor nectin-1 of herpes simplex virus 1 and/or herpes simplex virus 2 in normal and neoplastic human nervous system tissues. Acta Virol 2006;50:59–66. [PubMed: 16599187]
38. Valyi-Nagy T, Sheth V, Clement C, Tiwari V, Scanlan P, Kavouras JH, Leach L, Guzman-Hartman G, Dermody TS, Shukla D. Herpes simplex virus entry receptor nectin-1 is widely expressed in the murine eye. Curr Eye Res 2004;29:303–309. [PubMed: 15590476]
39. Ezra E, Pearson RV, Etchells DE, Gregor ZL. Delayed fellow eye involvement in acute retinal necrosis syndrome. Am J Ophthalmol 1995;120:115–117. [PubMed: 7611318]
40. Atherton SS, Streilein JW. Two waves of virus following anterior chamber inoculation of HSV-1. 1987. Ocul Immunol Inflamm 2007;15:195–204. [PubMed: 17613834]
41. LaVail JH, Tauscher AN, Sucher A, Harrabi O, Brandimarti R. Viral regulation of the long distance axonal transport of herpes simplex virus nucleocapsid. Neuroscience 2007;146:974–985. [PubMed: 17382478]

42. Smith LK, Kurz PA, Wilson DJ, Flaxel CJ, Rosenbaum JT. Two patients with the von Szily reaction: herpetic keratitis and contralateral retinal necrosis. Am J Ophthalmol 2007;143:536–538. [PubMed: 17317412]

43. Topp KS, Meade LB, LaVail JH. Microtubule polarity in the peripheral processes of trigeminal ganglion cells: relevance for the retrograde transport of herpes simplex virus. J Neurosci 1994;14:318–325. [PubMed: 8283239]

44. Butcher M, Raviprakash K, Ghosh HP. Acid pH-induced fusion of cells by herpes simplex virus glycoproteins gB and gD. J Biol Chem 1990;265:5862–5868. [PubMed: 2156833]

45. Kawakatsu T, Shimizu K, Honda T, Fukuhara T, Hoshino T, Takai Y. Trans-interactions of nectins induce formation of filopodia and lamellipodia through the respective activation of Cdc42 and Rac small G proteins. J Biol Chem 2002;277:50749–50755. [PubMed: 12379640]

Abbreviations

3-OS HS
3-O-sulfated heparan sulfate

3-OST-3
3-*O*-sulfotransferase-3

ARN
acute retinal necrosis

BFLA-1
bafilomycin A1

CF
corneal fibroblast

CHO-K1
Chinese hamster ovary-K1

Cyto D
cytochalasin D

FACS
fluorescence-activated cell sorter

FITC
fluorescein isothiocyanate

gB
glycoprotein B

gD
glycoprotein D

GFP
green fluorescent protein

gH
glycoprotein H

gL
glycoprotein L

HSV-1
herpes simplex virus 1

HSV-2
herpes simplex virus 2

HVEM
herpes virus entry mediator

Lat A
latrunculin A

MOI
multiplicity of infection

ONPG
o-nitrophenyl-β-D-galactopyranoside

PFU
plaque-forming units

RPE
retinal pigment epithelial

siRNA
small interfering RNA

X-gal
5-bromo-4-chloro-3-indolyl-β-D-galactopyranoside

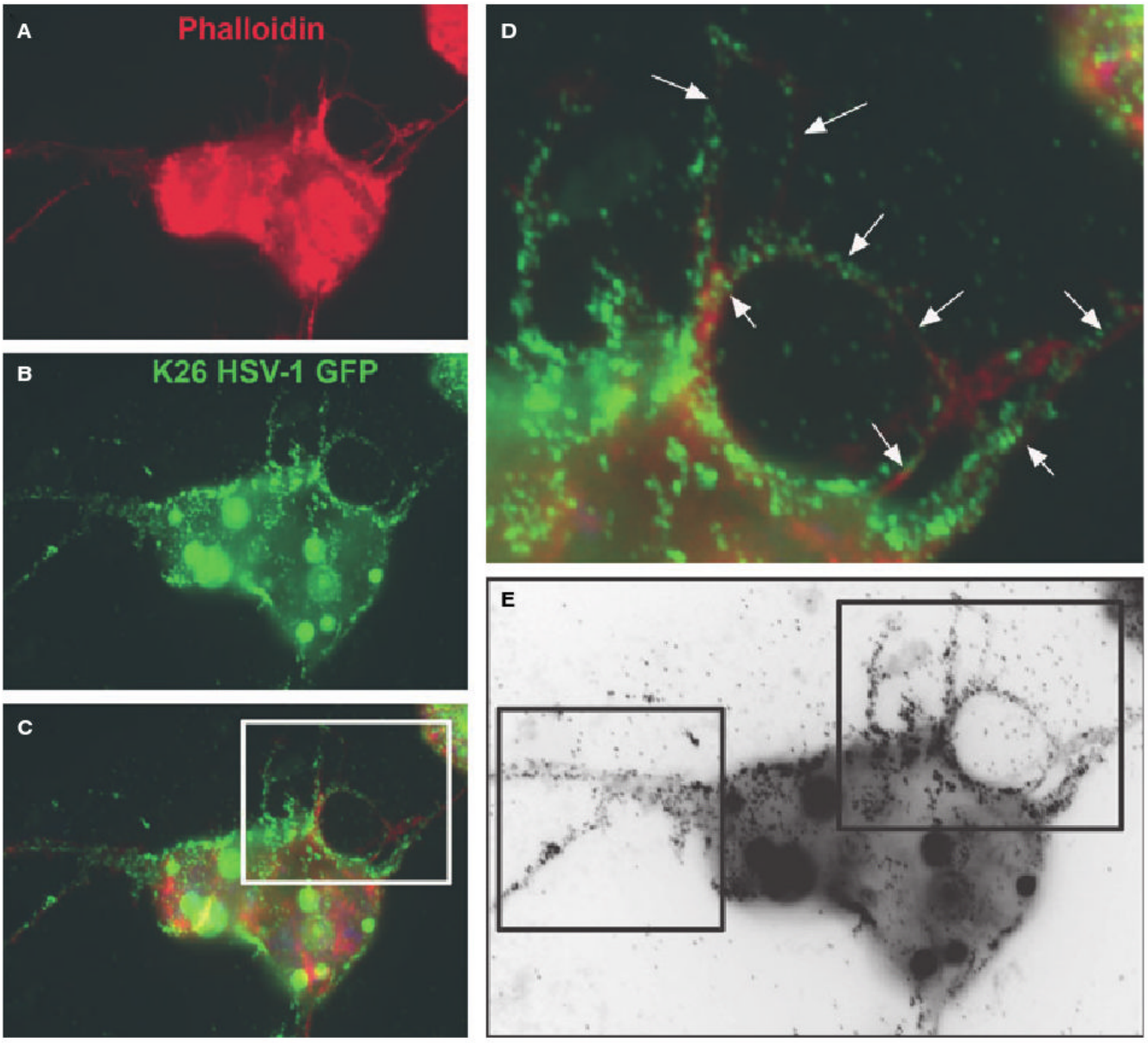

Fig. 1.

Binding of HSV-1 to filopodia. Cells were infected with HSV-1 (K26GFP) at 100 PFU per cell. The images were acquired at 30 min postinfection. (A) An infected RPE cell stained for actin (red) using phalloidin conjugated to rhodamine. (B) The same cell showing the virus particles (green). (C) The merged image demonstrates virus attachment to the cell body and filopodia. Arrows and boxes in (D) and (E) highlight the presence of the virus particles on filopodia-like structures.

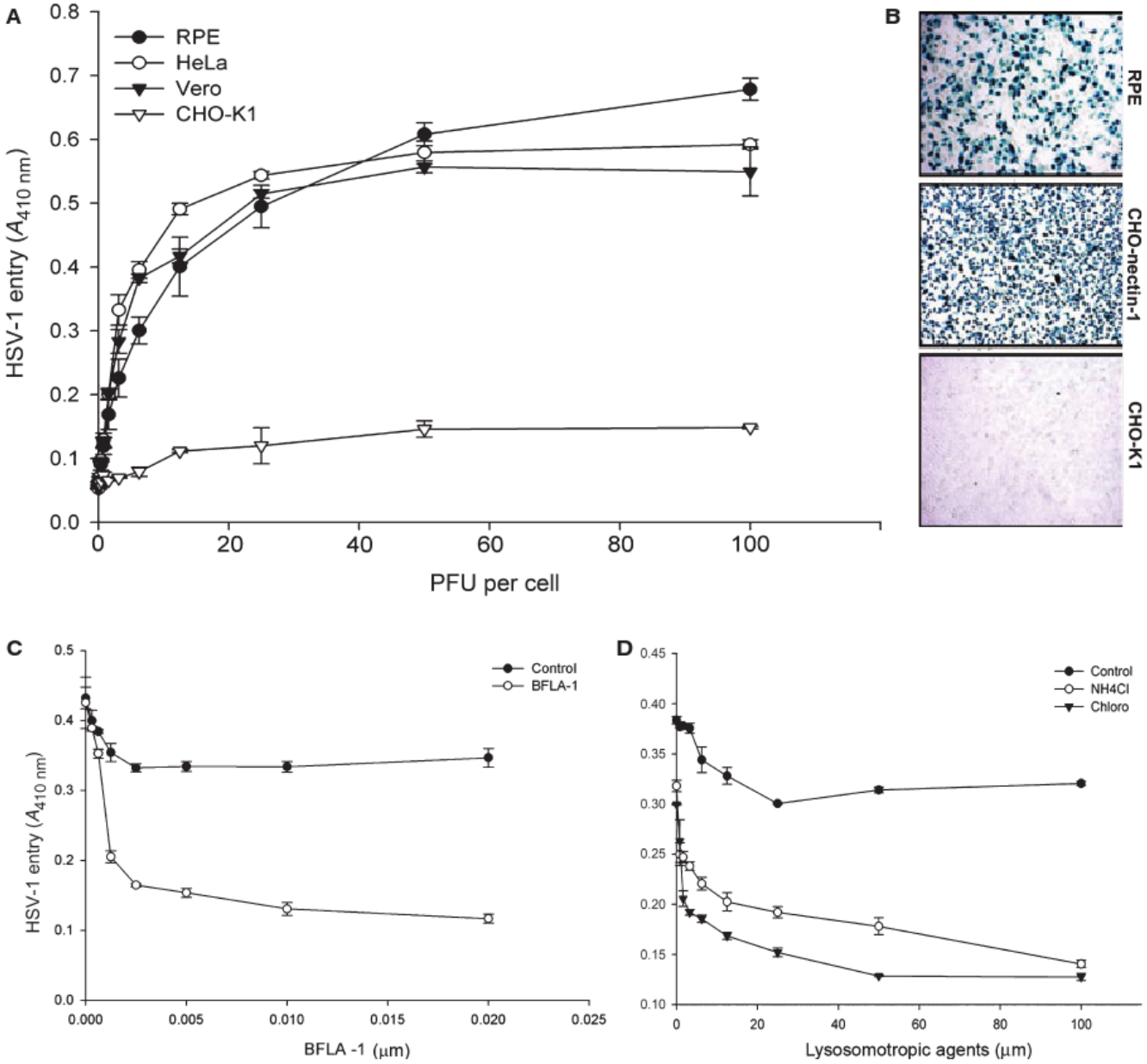

Fig. 2.

Entry of HSV-1 into RPE cells. (A) Dose–response curve of HSV-1 entry into RPE cells. Cultured RPE cells, along with cells naturally susceptible to HSV-1 (HeLa and Vero) were plated in 96-well plates and inoculated with two-fold serial dilutions of β-galactosidase-expressing recombinant virus HSV-1(KOS) tk12 at the PFU indicated. After 6 h, the enzymatic activity was measured at 410 nm. In this and other figures, each value shown is the mean of three or more determinations (± SD). HSV-1-resistant CHO-K1 cells were used as a control. (B) Confirmation of HSV-1 entry into RPE cells by X-gal staining. RPE cells grown (4×10^6 cells) in six-well dishes were challenged with β-galactosidase-expressing recombinant HSV-1 (gL86) at 20 PFU per cell. Wild-type CHO-K1 cells and nectin-1-expressing CHO-K1 cells were also infected in parallel as negative and positive controls. Blue cells (representing viral entry) were seen as shown. Microscopy was performed using the 20× objective of a Zeiss Axiovert 100. SLIDE BOOK version 3.0 was used for images. (C, D) HSV-1 entry into RPE

cells is pH-dependent. Monolayers of cultured RPE cells were pretreated with the indicated concentrations (μM) of the lysosomotropic agents BFLA-1 or chloroquine, or NH_4Cl, and exposed to HSV-1. Viral entry was quantitated 6 h after infection at 410 nm using a spectrophotometer. The mock-treated cells were used as a control.

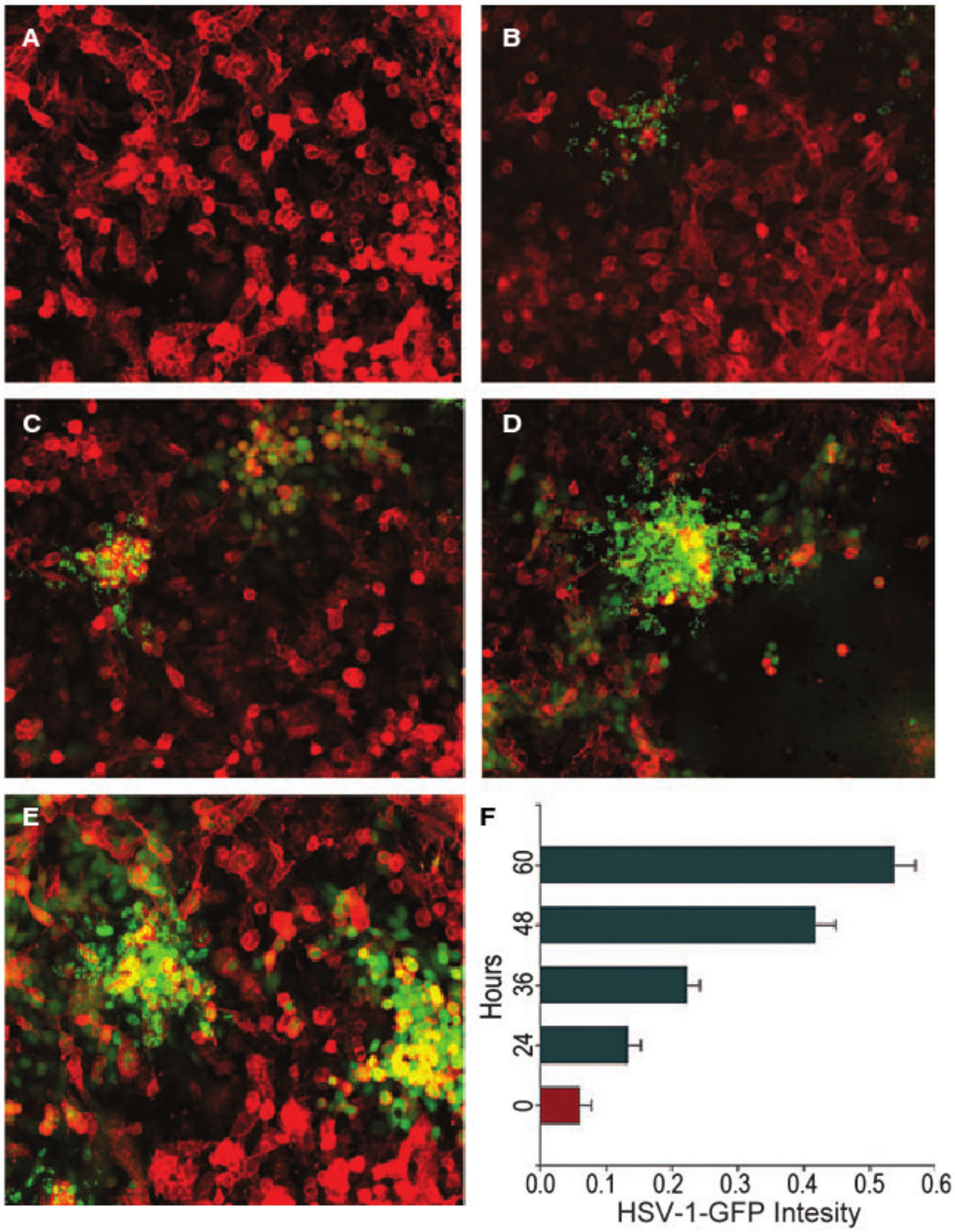

Fig. 3.

Imaging and quantification of HSV-1 replication in cultured RPE cells. Confluent monolayers of RPE cells were infected with K26GFP and the viral replication was imaged at (A) 0 h, (B) 24 h, (C) 36 h, (D) 48 h and (E) 60 h postinfection. In parallel, the same pools of cells were quantified for the increase in fluorescence intensity using a spectrophotometer (F). The GFP intensity increased exponentially over time, as seen in (A–E) and in graphical form in (F). The images were taken with a Zeiss Axiovert 100 microscope. Error bars represent standard deviations.

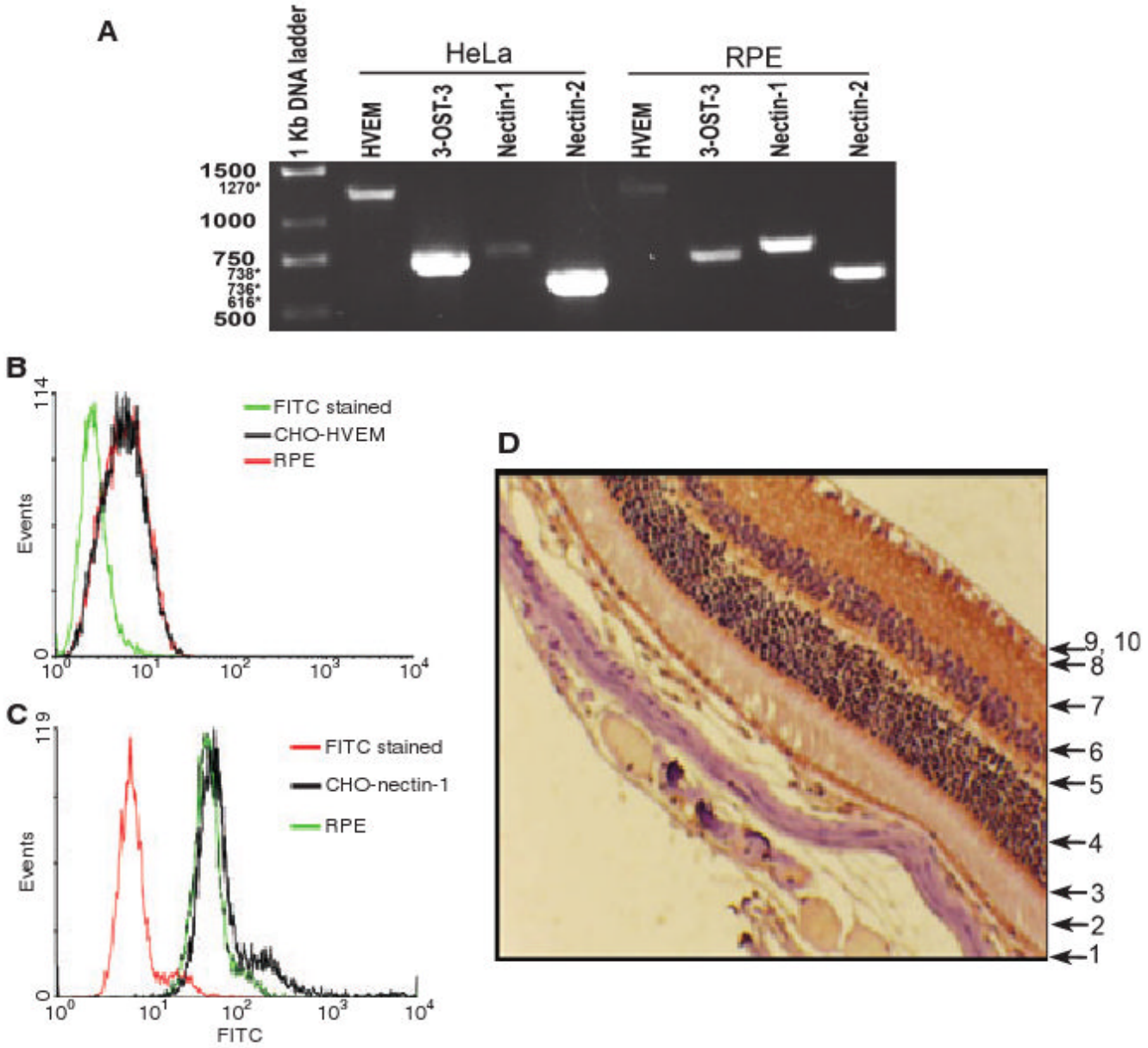

Fig. 4.

Expression of HSV-1 gD receptors in RPE cells. (A) RT-PCR analysis of the expression of HVEM, 3-OST-3, nectin-1 and nectin-2 in RPE and HeLa cells. The molecular mass markers are indicated on the left (sizes are in kilobases). Numbers with asterisks indicate expected sizes. (B, C) Cell surface expression of HVEM (B) and nectin-1 (C) in cultured RPE cells by fluorescence-activated cell sorter (FACS) analysis. Secondary antibody (FITC-stained)-treated cells were used as controls. (D) Nectin-1 expression in mouse tissue. Formalin-fixed, paraffin-embedded murine ocular tissues were sectioned and stained with a nectin-1-specific antiserum. Layers of the retina are marked by numbers as follows: 1, pigmented epithelial cells; 2, rod and cone processes; 3, outer limiting membrane; 4, outer nuclear layer; 5, outer plexiform layer; 6, inner nuclear layer; 7, inner plexiform layer; 8, ganglion cell layer; 9–10, optic nerve fibers and inner limiting membrane. Brown staining indicates nectin-1 expression.

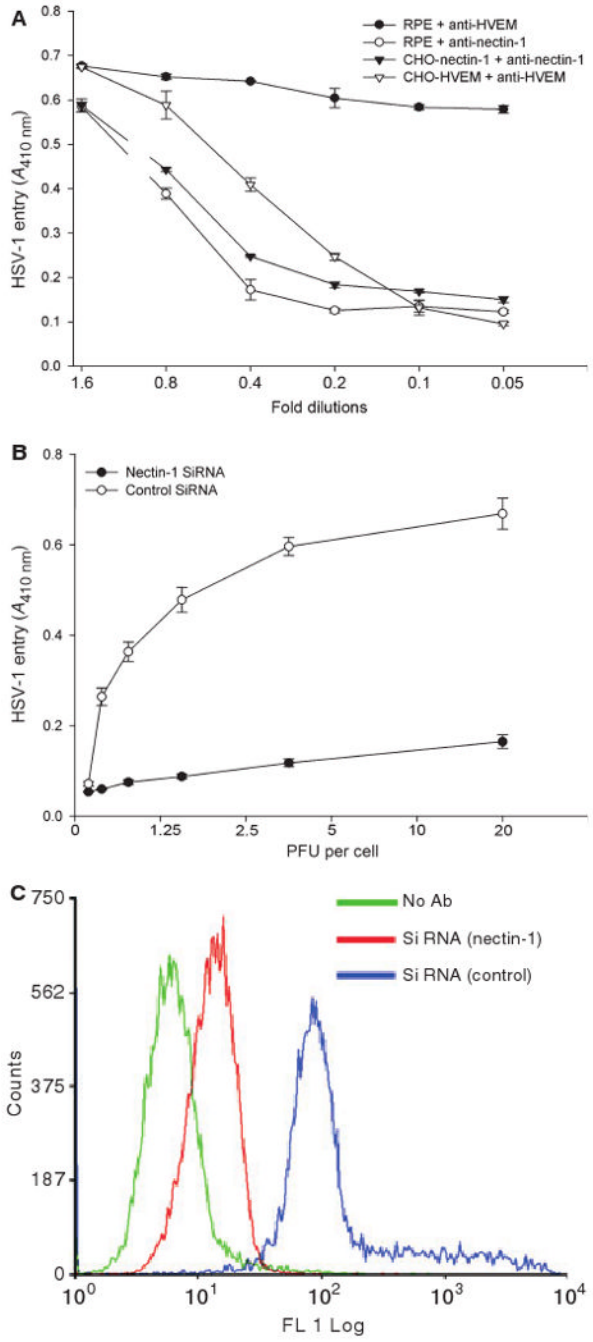

Fig. 5.

Role of nectin-1 during HSV-1 entry into RPE cells. (A) Antibody against nectin-1 significantly inhibits HSV-1 entry into cultured RPE cells. Cells (indicated) were incubated with twofold dilutions of the antibody against nectin-1 or with antibody against HVEM, and challenged with equal doses of HSV-1(KOS) gL86. β-Galactosidase activity was recorded 6 h later to determine entry. The experiment was repeated three times with similar results. (B) Knocking down of nectin-1 expression in RPE cells significantly blocks HSV-1 entry. Specific siRNA against nectin-1 and a control siRNA were transfected into RPE cells, and the cells were then challenged with a two-fold dilution of HSV-1(KOS) gL86. β-Galactosidase activity at 6 h postinfection is shown. (C) Cell surface expression of nectin-1 in RPE cells is downregulated

by the siRNA. Monolayers of RPE cells were either mock transfected or transfected with siRNA against nectin-1 or control siRNA. Sixteen hours later, cells were incubated with nectin-1 antibody (R65), stained with FITC-conjugated secondary anti-(rabbit IgG), and analyzed by FACS. RPE cells stained with FITC-conjugated secondary anti-(rabbit IgG) were used as a background control.

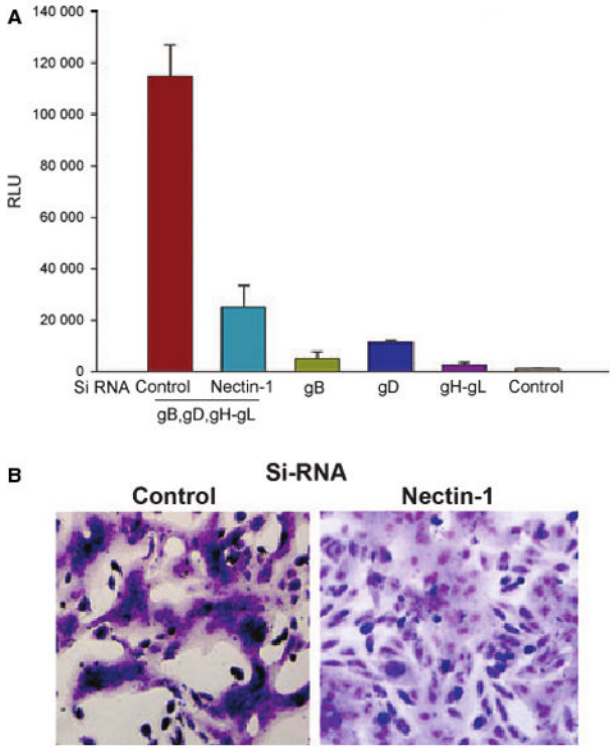

Fig. 6.

Role of nectin-1 in HSV-1-induced fusion of RPE cells. (A) Membrane fusion of RPE cells requires nectin-1 and the presence gB, gD, gH and gL. The 'target' RPE cells were transfected with either a control or nectin-1-specific siRNA. The 'effector CHO-K1 cells' were transfected with expression plasmids for the HSV-1 glycoproteins indicated, and mixed with 'target RPE cells'. Membrane fusion as a means of viral spread was detected by monitoring luciferase activity. Relative luciferase units (RLUs), determined using a Sirius luminometer (Berthold detection systems), are shown. Error bars represent standard deviations. *$P < 0.05$, one-way ANOVA. (B) Downregulation of nectin-1 inhibits HSV-1-induced cell-to-cell fusion. The 'effector CHO-K1 cells' were mixed with either control (B, left panel) or nectin-1-specific siRNA-transfected (B, right panel) 'target RPE cells'. At 18 h postmixing, the cells were fixed and stained with Giemsa to demonstrate syncytia formation.

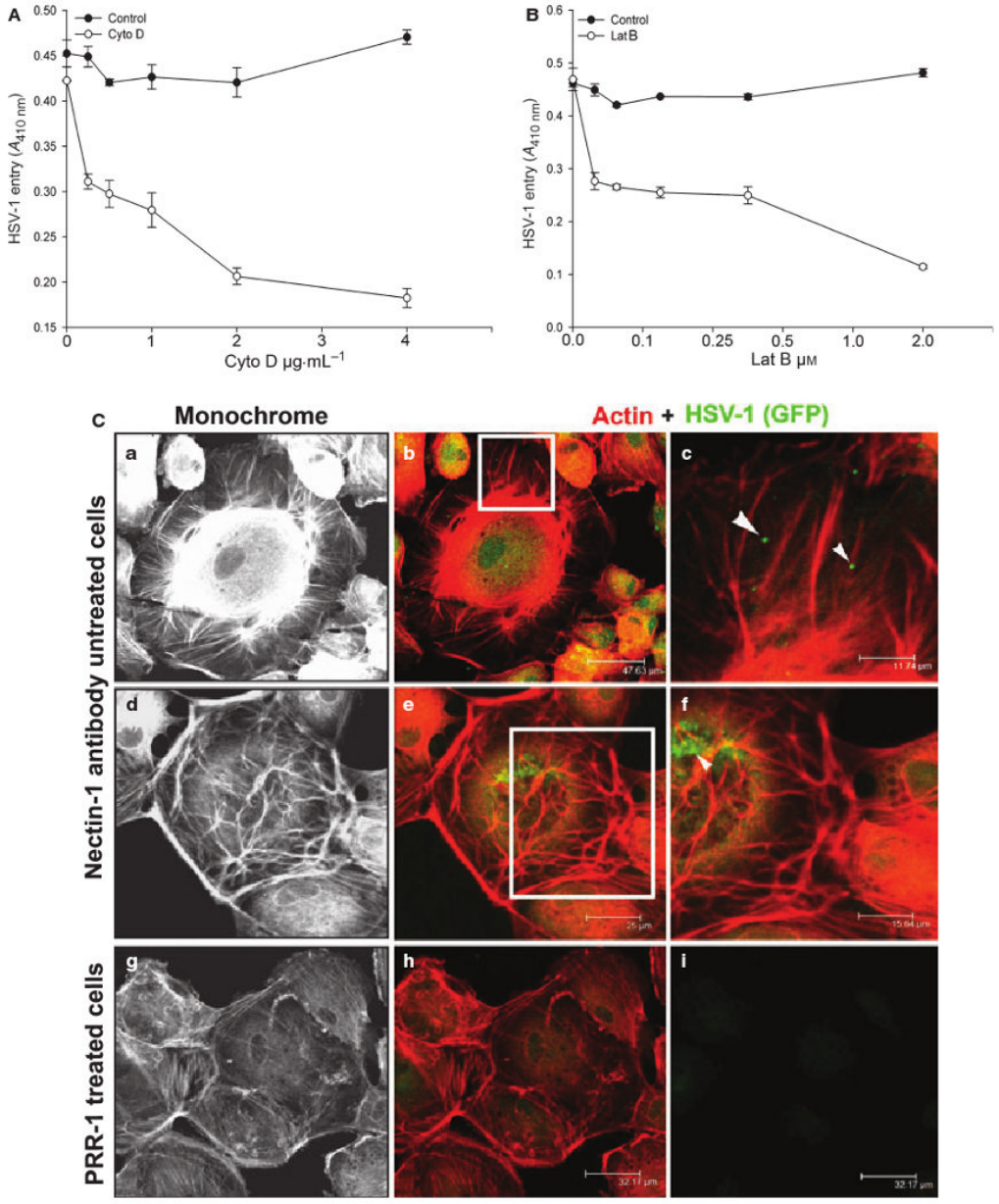

Fig. 7.

Actin depolymerizers block HSV-1 entry into RPE cells. (A, B) Monolayers of cultured RPE cells were pretreated with the indicated concentrations of the actin-depolymerizing agents, Cyto D and Lat A, and exposed to HSV-1 (50 PFU per cell). The mock-treated RPE cells were used as a control. Viral entry was quantified 6 h after infection at 410 nm, using a spectrophotometer. (C) Nectin-1 antibody significantly reduces the changes in actin cytoskeleton in RPE cells. (a)–(f) Changes in the actin cytoskeleton in HSV-1-infected RPE cells. The boxed regions in (b) and (e) are highlighted in (c) and (f). Arrows and arrowheads in (c) and (f) indicate the association of HSV-1 GFP particles with actin-stained rhodamine phalloidin. (g, h) Effect of nectin-1 antibody (PRR1) treatment on HSV-1 GFP-infected RPE cells. (i) The presence of HSV-1 GFP on RPE cells. All pictures were taken with a confocal microscope at 40× magnification.